J. Appl. Glycosci., **68**, 77–87 (2021)
doi: 10.5458/jag.jag.JAG-2021_0009

Regular Paper

"Nata Puree," a Novel Food Material for Upgrading Vegetable Powders, Made by Bacterial Cellulose Gel Disintegration in the Presence of (1,3)(1,4)-β-Glucan

(Received June 30, 2021; Accepted September 28, 2021)
(J-STAGE Advance Published Date: October 4, 2021)

Ken Tokuyasu,[1,†] Kenji Yamagishi,[1] Junko Matsuki,[1] Daisuke Nei,[1] Tomoko Sasaki,[1] and Masakazu Ike[1]

[1] *Food Research Institute, National Agriculture and Food Research Organization*
(*2–1–12 Kannondai, Tsukuba, Ibaraki 305–8642, Japan*)

Abstract: Pulverization is a potentially powerful solution for the resource management of surplus- and non-standard agricultural products, maintaining their nutritional values for long and ensuring their homogeneity, whereas their original textures could disappear to narrow the application ranges. Therefore, new technologies should be developed for reconstructing the powders to provide them with new physical characteristics. Herein, we developed a novel food material, nata puree (NP), by nata de coco (bacterial cellulose gel) disintegration with a water-soluble polysaccharide using a household blender. The process worked well with (1,3)(1,4)-β-glucan (BGL) as the polysaccharide, which could be substituted with barley extract. Lichenase treatment of the NP dramatically modified its physical properties, suggesting the importance of the BGL polymeric forms. NP exhibited distinct potato powder and starch binding activities, which would be attributed to its interactions with the cell wall components and a physical capture of powders by the NP network, respectively. NP supplementation into the potato paste improved its firmness and enabled its printable range shift for 3D food printing to a lower powder-concentration. NP also promoted the dispersion of powders in its suspension, and designed gelation could also be successfully performed by the laser irradiation of an NP suspension containing dispersed curdlan and turmeric powders. Therefore, NP could be applied as a powder modifier to a wide range of products in both conventional cooking, food manufacturing, and next generation processes such as 3D food printing.

Key words: (1,3)(1,4)-β-glucan, nata puree, bacterial cellulose gel disintegration, vegetable powders, 3D food printing

INTRODUCTION

A report jointly prepared by the international organizations in 2020 describes that two billion people have experienced food insecurity at either a severe or moderate level, reflecting the current situation that food security has been threatened by the growing world population, as well as other factors, such as climate change and emerging infectious diseases.[1)2)3)] Regarding this problem, a big contradiction is that 14 % of the global food production (on an economic weight basis) has been abandoned as food loss,[4)] while 688 million people in the world are estimated to have been undernourished in 2019.[1)] Therefore, it would be pivotal to reduce food loss by upgrading the abandoned foods that are still edible and putting them back in the chain. Particularly, surplus- and non-standard agricultural products of plant origin (*i.e.*, vegetables, fruits, roots, tubers, *etc.*) are expectedly the superior resources for upgrading to those decayed and those at premature or overripened stage as they could display the same safety levels as the corresponding products for the market and contain the equivalent nutritional values and functional components. Meanwhile, those resources generally exhibit problems in their very short shelf lives in the wet forms and/or the heterogeneity enough to be categorized as non-standard.

Pulverization of the agricultural products to prepare dry powders is a promising solution to the aforementioned problem as it could ideally extend product shelf lives by the reduction of water-related activities without the significant loss of nutritive, functional, taste-, flavor-, and color-related values.[5)6)] In addition, it could transform the heterogenous agricultural products into homogeneous powders, which is advantageous for the formulation of processed foods with controlled constituents in quantity.[5)] This concept can also be a breakthrough for upgrading unpopular food resources (like insects) or visually unpleasant foods for consumption (like by-products of food processing) into nutritious food powders of different structures from those of the originals.[5)7)] Homogeneous powders are also expected to be applied in the three-dimensional (3D) food printing as the next-generation cooking machine, which would guarantee

†Corresponding author (Tel. +81–29–838–7300, Fax. +81–29–838–7996, E-mail: tokuyasu@affrc.go.jp).
Abbreviations: NP, nata puree; BGL, (1,3)(1,4)-β-glucan; BE, barley extract; BC, bacterial cellulose; OD, optical density; RVA, Rapid Visco Analyzer; NP*, standard NP sample made with BGL; NPw, disintegrated BC sample with water; NPbe, NP sample made with BE.

high reproducibility of the 3D structures according to digital programs.[7)]

However, the pulverization of fresh vegetables or fruits has a large drawback in that the process diminishes the well-accustomed, unique textures by the disruption of the 3D structures. For example, the crispy texture of fresh cabbage significantly reduces when powdered. Textures of fresh foods or those expressed through their cooking processes are among the most important factors that determine the palatability of foods, the ranges of application, and the commercial values.[8)] Therefore, in order to regain this potentiality, it is important to develop new textures that are expressed based on the characteristics of individual food powders. Except for certain excellent gel-forming powders, such as starchy powders and konjac powders to generate unique textures by cooking or processing, most vegetable- or fruit-derived powders have insufficient amounts of gel-forming components. Instead, primary cell wall components such as pectin, hemicellulose, and cellulose, would be exposed at the surface of the powders.

In this study, we developed a novel food material that interacts with such cell-wall components to bridge the powders and help construct new paste products or suspensions. The material could be readily made by mechanical shearing of nata de coco in the presence of (1,3)(1,4)-β-glucan (BGL) or barley extract (BE) rich in BGL. Nata de coco is a traditional fermented food, produced by certain strains of acetic acid bacteria as a gel made of bacterial cellulose (BC).[9)10)] Disintegrated products of nata de coco reportedly impart various physical properties in foods.[11)12)13)] However, this disintegration could only be achieved under harsh conditions by specific instruments such as high-pressure homogenizers and ultrasound devices,[12)13)14)15)] which could be barriers to a wider application of the disintegration product. We inclusively termed "nata puree (NP)" the materials produced by the BC gel disintegration in the presence of a water-soluble polysaccharide, such as BGL. Since the 3D food printing technology is expected to produce new textures to food powders through the fine control of 3D structures,[7)] the characteristics of NP-blended paste samples and suspensions with food powders were also analyzed regarding the application to unit processes in 3D food printing. The content of this article is divided into two parts. The first focuses on the preparation and basic properties of NP, and the second deals with the interactions of NP with food materials and their application.

MATERIALS AND METHODS

Materials. Nata de coco (Morinaga nata de coco plain) was purchased from Morinaga Milk Industry Co., Ltd., Tokyo, Japan. BGL (P-BGH, high viscosity, Megazyme), lichenase (endo-1,3:1,4-β-D-glucanase: E-LICHN, Megazyme; 273 U/mg protein), and xylanase (endo-1,4-β-xylanase: E-XYNACJ, Megazyme; 38 U/mg protein) were purchased from Biocon (Japan) Ltd., Nagoya, Japan. Barley grain was purchased from Hakubaku Ltd., Chuo, Japan. Potato powders were purchased from Syunsai-Kobo KOKORO, Yokkaichi, Japan. Potato starch and turmeric powders were purchased at a domestic supermarket. Other chemicals were of the reagent grade.

Preparation of NP samples. Since the purchased nata de coco was preserved in syrup, it was repeatedly soaked in excess water to remove sugar (de-syrup) in the gel. That is, nata de coco gel (4 kg) was soaked in 16 L of tap water and agitated gently with a rotary blade at 100 rpm. The water was replaced with fresh water every day for a week. The de-syrupped nata de coco was preserved at 4 ℃ until use. The preparation of NP from the de-syrupped nata de coco and BGL was performed as follows: BGL was dispersed in 40 mL of water (0.7 % w/v), and the suspension was boiled by microwave to dissolve BGL. The BGL solution was cooled to room temperature and mixed with 100 g of the de-syrupped nata de coco. The mixture was blended to disintegrate the de-syrupped nata de coco using a power blender (Cuisinart SPB-650J, Conair Japan, Tokyo, Japan) at 9,000 rpm for 30 s. The disintegration was repeated three more times, and this NP sample was defined as the standard NP sample (NP*). For certain experiments, the BGL concentration or the time (the number of 30-s blending) for blending was modified. The sample made under the corresponding condition for disintegration without BGL was termed NPw. The barley extract (BE) was prepared as follows: barley grains were milled (1-mm mesh pass) with a Wiley Mill (SRG 05C, SATAKE Corporation, Higashi-Hiroshima, Japan), and the powders were heated at 80 ℃ for 18 h for enzyme inactivation. Then, the heat-treated powders were cooled to room temperature and mixed with distilled water at a ratio of 1 to 5 (w/v). The mixture was shaken at 200 rpm for 1 h at 40 ℃ and centrifuged at 8,000 × G for 10 min. The supernatant was then taken and centrifuged at 26,000 × G for 10 min, and the supernatant of the second centrifugation was used as BE. The BGL concentration in the BE was measured using the Megazyme β-Glucan Assay Kit (K-BGLU, Biocon (Japan)). Forty milllitters of BE was used for NP preparation following the same procedure as that of the 0.7 % BGL solution described above. The sample of NP made with BE under the standard condition for disintegration was termed NPbe. The BE enzymatic treatment was done as follows: 100 U of lichenase or 50 U of xylanase were added to 40 mL of BE (adjusted at pH 5.6 with sodium phosphate buffer to a final concentration of 25 mM), and the mixture was shaken at 100 rpm and 60 ℃ for 2 h, then these solutions were mixed with 100 g of de-syrupped nata de coco for preparation of NP as described above.

Particle size distribution analysis with a testing sieve. Individual NP samples prepared with distilled water, BGL, BE, and enzyme-pretreated BE were diluted 5 times with distilled water (w/v), then the diluted samples were gently stirred for 3 min. The optical density (OD) at 600 nm ($OD_{600\ nm}$) of each suspension was measured using a spectrophotometer (SpectraMax Plus 394, Molecular Device Japan, Tokyo, Japan) with 1-mL cuvettes with a path length of 10 mm. The measurements were repeated four times, and the average value was calculated. Then, the suspensions (40 mL) were poured onto either of the two testing sieves (apertures: 500 and 300 μm, respectively; diame-

ter: 75 mm, Tokyo Screen, Co., Ltd., Tokyo, Japan). The $OD_{600\ nm}$ of the filtrates were measured as described above. All these procedures were done twice, and the average value of the two experiments and standard deviation were calculated for each suspension.

Particle size distribution analysis with particle size analyzer. Three types of NP samples were prepared using 100 g of BC and 40 mL of BGL solution (0.7 % w/v) by setting the disintegration times to a total of 2 (*i.e*., NP*), 4, and 6 min, respectively. These NP samples were diluted 5 times with distilled water as described above, and the particle size distribution of each sample was analyzed by a particle size analyzer (LS13 320, Beckman Coulter K.K., Tokyo, Japan).

Rheological analyses. The BC sample rheological properties were determined using a dynamic rheometer (HAAKE MARS iQ, Thermo Fisher Scientific Inc., Waltham, MA, USA) with a cone-plate geometry as follows: cone angle of 2° and diameter of 35 mm. The shear viscosity was measured using a shear rate sweep test at 25 °C. The shear rate was increased from 0.01 to 10 s^{-1}. The storage modulus (G′) and loss modulus (G″) of the samples were measured using oscillatory time sweep mode at a frequency of 1 Hz and 0.1 % strain within the linear viscoelastic region for 5 min (25 °C). Four kinds of samples were examined for the analysis: NPw, NP*, a sample prepared by the treatment of NP* with lichenase, and NPbe. The NP* lichenase treatment was performed as follows: lichenase (20 U) was added to 20 g of NP* in a plastic tube, and the tube was shaken at 200 rpm and 40 °C for 3 h. All samples were measured in triplicates.

The pasting properties were analyzed using a Rapid Visco Analyzer (RVA) (model RVA4, Newport Scientific Pty. Ltd., Warriewood, Australia). The powder suspension was prepared by adding 3.0 g of potato powder or 2.0 g of potato starch to a canister containing 25.0 mL of water or a diluted NP* suspension (solid content of 0.344 % (w/v)) and mixing thoroughly by jogging the paddle vigorously. The viscosity profile was recorded using the Thermocline software for Windows under the conditions as follows: each suspension was kept at 50 °C for 1 min, heated up to 95 °C in 3.7 min, held for 2.5 min at 95 °C, cooled to 50 °C in 3.8 min, and kept for 2 min at 50 °C. The paddle was constantly rotated at the speed of 160 rpm. The peak viscosity, pasting temperature, and peak time were recorded.

The NP addition effects on the physical properties of potato paste samples were investigated using a rheometer (CR-500DX, Sun Scientific Co., Ltd., Tokyo, Japan). Six samples of potato powders (28 g/sample, water content 10.6 % (w/w)) were individually mixed with 72 g of water, NPw, NP*, NPbe, 0.2 % (w/v) BGL solution, and BE suspension (containing 0.2 % (w/v) BGL), respectively. Three plastic dishes (diameter: 50 mm, height: 10 mm) were filled each with a separate paste sample of each kind (27 g for one dish) for analysis. The analytical parameters were obtained according to a previous report:[16] that is, a cylindrical plastic plunger (diameter: 10 mm, height: 20 mm) was lowered into contact with the top of the sample and further penetrated to a depth of 2.5 mm at a speed of 1 mm/s. Then, the plunger was lifted at the same speed, and the force *vs*. time was plotted. The firmness peak, adhesiveness peak, adhesiveness area, and extension length were calculated.[17]

Powder dispersion analysis. Potato powders (50 mg) were added to individual tubes containing 1.4 mL of water or NP* suspensions (the solid content of 0.197, 0.049, or 0.012 %), the suspensions were mixed well, and the tubes were settled at room temperature for 1 h. As a different series, potato starch powders (50 or 400 mg) were added to individual tubes containing 1.4 mL of water and NP* suspension (solid content of 0.197 or 0.388 %), the suspensions were mixed well, and the tubes were also settled at room temperature for 1 h. Then, the powder dispersions in the tubes were observed.

Printing with 3D food printer. A 3D food printer equipped with a screw type extruder (FP-2500, Seiki Co. Ltd., Yamagata, Japan) was used in this study. Paste samples of potato powders with and without NPbe were prepared at room temperature right before filling them in a reservoir in the 3D food printer. Thirty-five grams of potato powder (equivalent to 31.3 g dry weight) were mixed with 123 g of NPbe to adjust the potato powder content (as dry matter) to 20 % (w/w). The same potato powder weights were individually mixed with 123 and 104 g of distilled water to adjust the potato powder contents to 20 and 22.5 % (w/w), respectively. A 3D design of the cylinder (diameter, 3 cm; height, 3 cm) was created using an open-source software (FreeCAD), and the modeling data was processed by an open-source slicer (Slic3r) to make a G-code for the printer. The nozzle diameter was 2.0 mm, and the extrusion multiplier and the print speed at room temperature were 4.0 and 15.0 mm/s, respectively. The distance between the nozzle and the printing stage was kept at 1.0 mm and the infill percent was set at 100 %. After the printing process, the diameters at the bottom of the products were calculated.

Gel formation experiments. One milliliter of water or NP* suspension (the solid content of 0.172 %) was mixed with the same volume of 4 % (w/v) suspension of curdlan powders in a test tube. Each tube was heated to 85 ºC for 15 min and settled at the bench to cool to room temperature without agitation. Then, each test tube was tilted to observe the fluidization and the extent of gelation.

For the gel formation experiment by laser irradiation, 50 mg of turmeric powder was dispersed to the 2 mL of NP*/curdlan suspension described above. The mixture was spread on a glass plate, and it was irradiated from the top of the sample with a blue laser light (laser power: 3 W, wavelength: 450 nm) for the printing of four characters N, A, R, and O (Fig. S1; see J. Appl. Glycosci. Web site) using the Small Laser Engraving Machine J3 (Dongguan Diaojiang Technology Co., Ltd., Dongguan, China). The parameters of the laser power and carving depth were set at 100 and 60 %, respectively. After the irradiation step, the sample was rinsed with deionized water to identify the shape of the gel.

Statistics. Calculation for statistical analysis using unpaired Student's *t*-test was performed with the software Microsoft Excel for Office 365 MSO (Microsoft Corp., Redmond,

WA, USA). Differences were considered significant at $p < 0.05$.

RESULTS AND DISCUSSION

NP preparation and characterization.

The disintegration of the de-syrupped nata de coco in the presence of BGL or BE was evaluated by the change in turbidity before and after passing through a stainless mesh filter with a pore diameter of 500 or 300 μm (Fig. 1). In the presence of 0.2 % BGL, 73.6 and 53.7 % of particles in the NP* sample passed filters of 500 and 300 μm pore size, respectively. The solid NP* content was 0.688 % (w/v). In contrast, the conditions with BGL at 0.1 and 0 % (*i.e.*, NPw) were significantly less effective, and flocs were observed by a visual judgment, suggesting that the disintegration was insufficient in those cases.

A similar disintegration effect to that of BGL was obtained when BE of the same BGL content was used. When lichenase, which specifically decomposes BGL, was added to BE prior to disintegration, the disintegration efficiency dramatically decreased. It suggests that a part of the disintegration promoting effect in BE would be attributed to polymeric BGL. Similarly, the xylanase (xylan decomposer) pretreatment of BE also reduced the disintegration, suggesting that polymeric xylan would also, at least in part, contribute to the disintegration.

The filtration method used for the evaluation in Fig. 1 is simple for predicting the degree of disintegration, whereas it should be noted that the well-disintegrated NP organizes a highly water-retaining network, held on the mesh (data not shown). In that case, the recovery rate of the mesh-passing fraction decreases even though the disintegration appears to be successful. The visual confirmation of the presence of flocs in the NP should help judge the disintegration efficiency, and only NP* and NPbe samples in Fig. 1 were visually confirmed as well-disintegrated with few flocs.

Figure 2 shows the changes in particle size distributions when the disintegration time was extended from 2 min to 4 or 6 min. In the 2-min disintegrated sample (*i.e.*, NP*), only one broad area of diameters between 8.94–1,820 μm was present. In contrast, multiple peaks appeared in a 4-min disintegrated sample at diameters between 5.11–1,510

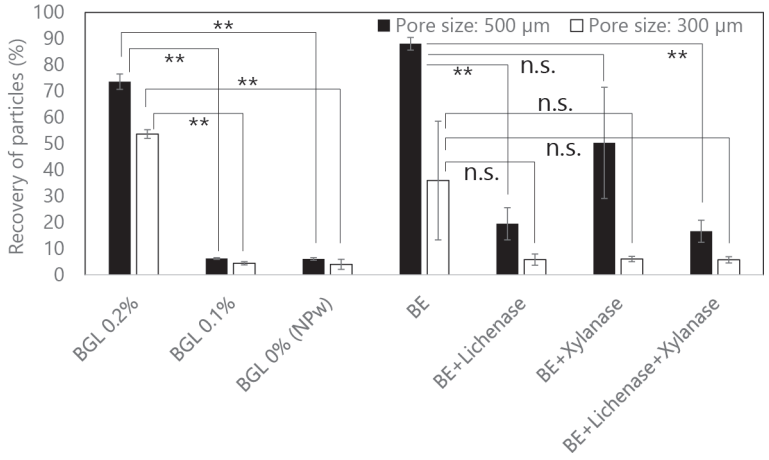

Fig. 1. Changes in turbidities of disintegrated BC samples by passing through filters.

Turbidity was measured as the $OD_{600\ nm}$, and the ratio of turbidity after passing through 500 and 300 μm filters to that before filtration is indicated. Results were expressed as means ± SD. Statistical analysis was performed using unpaired Student's *t*-test; $p < 0.05$ was considered statistically significant ($^{*}p < 0.05$, $^{**}p < 0.01$, n.s.; no significance).

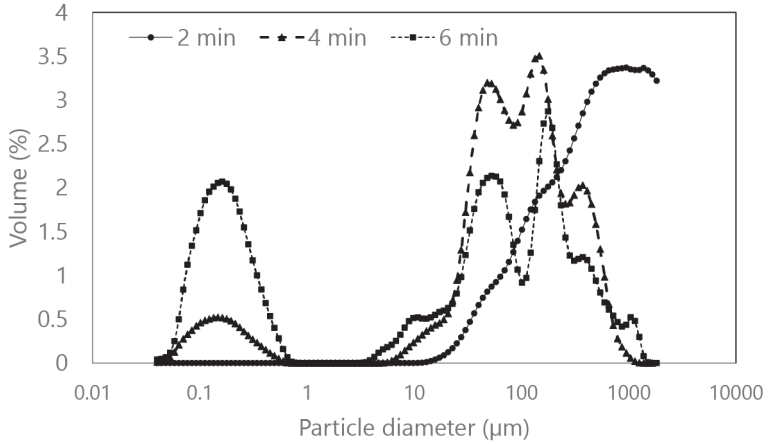

Fig. 2. Particle size distribution of disintegrated BC in the presence of BGL.

Sample data of disintegration times of 2, 4, 6 min are shown as a solid line with circles, bold broken line with triangles, and broken line with squares, respectively.

μm as well as a new single peak at those between 0.040–0.868 μm. A similar trend was observed in a 6-min disintegrated sample with multiple peaks at diameters between 2.92–1,510 μm and a single peak at those between 0.040–0.791 μm. The peak shift to the left side of the figure with the prolonged disintegration time suggests that the disintegration step worked well with a household blender. It was reported that the particle size of disintegrated bacterial cellulose with a household homogenizer reaches a level-off stage after a 1-min treatment, suggesting that BGL positively affected the disintegration in our study.[18] The corresponding peak areas at diameters over 1 μm in 4- and 6-min disintegrated samples were composed of multiple small peaks. In addition, one peak could be observed at the submicron range at 0.040–0.868 μm in 4-min disintegrated sample or 0.04–0.791 μm in 6-min disintegrated sample, and the volume ratio increased after a prolonged disintegration. These unique profiles would be attributed to multiple factors in both the BC sample and disintegration conditions: the BC biosynthesis conditions significantly affected the distribution of BC polymerization as well as the morphology and the disintegration with shearing power tears off BC into anisotropic particles with well-oriented fibers.[18] The possibility that the peaks in the submicron range could originate from BGL was excluded by the analysis of the BGL solution to find no detectable peaks at the submicron range (data not shown).

Figure 3 shows the shear stress and the apparent viscosity comparison of the NP samples as a function of shear rate. All the samples exhibited a shear stress increase (Fig. 3A) and shear-thinning behavior (Fig. 3B) when the shear rate was increased from 0.01 to 10 s^{-1}, which has been already reported in the other BC-related study.[15] The BGL and BE supplementation decreased the viscosity of the BC suspensions, and BE showed a higher impact on the viscosity of BC suspensions. The NP* sample after the treatment with lichenase showed a similar viscosity curve profile to NPw. Figure 4 compares the viscoelastic parameters of the NP samples. The BGL and BE supplementation dramatically decreased the G′ and G″ values, and the effect was emphasized when BE was added. The NP* sample after treatment with lichenase showed similar G′ and G″ values to NPw. These results indicate that the BGL and BE supplementation reduced both the elastic and viscous components of the BC samples. As described above, the NPw sample appeared to be less homogenous with flocs

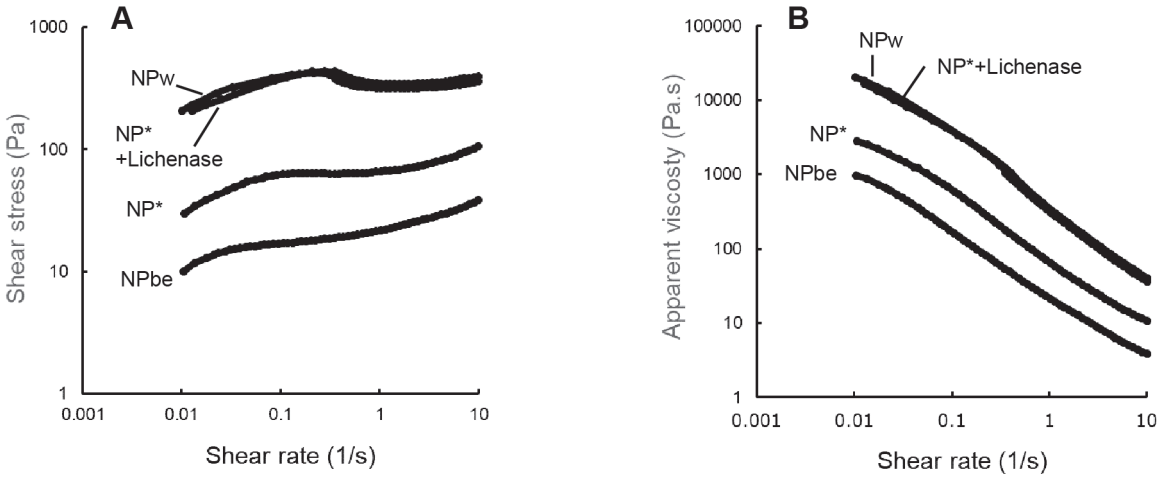

Fig. 3. Shear stress (A) and apparent viscosity (B) of the BC samples as a function of shear rate.
NPw, NP*, a sample prepared by the treatment of NP* with lichenase, and NPbe were examined for the analysis.

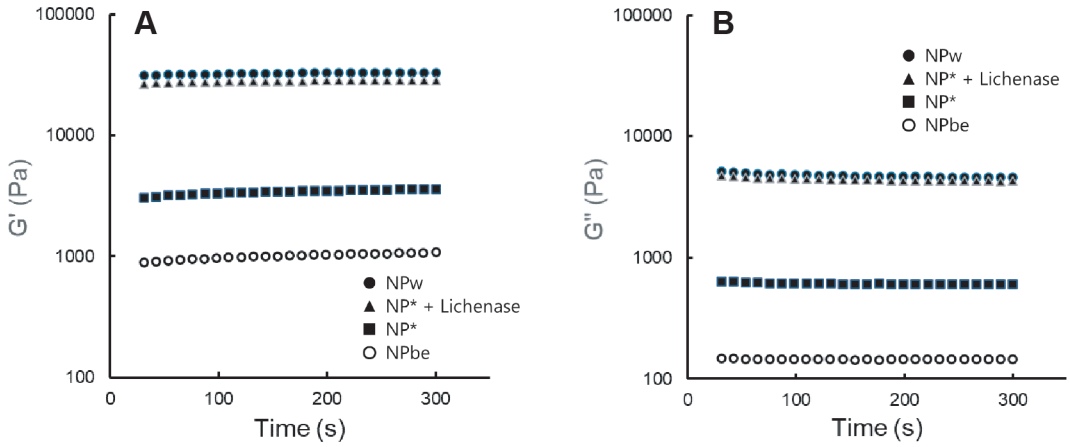

Fig. 4. Storage modulus (A) and loss modulus (B) of the BC samples as a function of time.
NPw, NP*, a sample prepared by the treatment of NP* with lichenase, and NPbe were examined for the analysis.

than NP* and NPbe, suggesting that suspension homogeneity might influence the rheological properties.

In this study, we hypothesized that the inefficient BC disintegration in previous reports[14)18)] would be attributed to the strong interaction of the newly exposed cellulose fibers with the neighboring cellulose surfaces in the same floc during the disintegration process. This strong interaction would result in a rapid reunion of the fiber with a very close cellulose surface in the same floc, resulting in a delay of the disintegration into smaller flocs. We also speculated that BC disintegration in the presence of water-soluble polysaccharides (such as BGL) with activities to interact with the cellulose surface, could competitively bind to the newly exposed cellulose fibers and thus suppress the new cellulose-cellulose interaction as a possible cause of inefficient disintegration. Results in Fig. 1 supports our hypothesis and speculation, and xylan in BE would also be effective in the promotion of disintegration. A similar disintegration effect could be observed when other polysaccharides such as xyloglucan, xylan derivatives, guar gum, carboxymethyl cellulose salt, sodium alginate, and chitosan were applied instead of BGL (data not shown). Further analysis would be required for the disintegration optimization, including an observation of the surface structures of NP and an analysis of the binding properties of water-soluble polysaccharides to BC during the disintegration.

Synthetic research on polysaccharide-polysaccharide interactions has been performed by the characterization of BC derivatives through the supplementation of the medium for the BC biosynthesis with water-soluble polysaccharides such as BGL, arabinoxylan, and xyloglucan.[19)20)] These water-soluble polysaccharides interact with cellulose during the biosynthesis and are incorporated into BC to modify the properties of the composites. In addition, unique activities of the bound BGL on cellulose were reported, including the promotion of arabinan and galactan binding with BGL-bound cellulose[21)] and a water-structuring coadjuvant activity for cellulose.[22)] However, to the best of our knowledge, no study reports that these polysaccharides would show excellent BC disintegration properties.

BGL is a hemicellulose type found mainly in the primary cell wall of gramineous plants.[23)] BGL is known to be present in grains such as barley, oats, wheat and rice. It serves as a dietary fiber and exhibits metabolic activities when appropriately taken.[24)] BGL is readily extracted with water from the aforementioned grains, and our NP preparation process with a household blender makes it possible to obtain NP in kitchens for cooking at home and small restaurants, as well as for food manufacturing. Meanwhile, since grains have endogenous BGL-degrading enzymes, those enzymes should be inactivated beforehand when the grain or flour is used for extraction or as powders or granular materials of grains are mixed with NP including BGL.

Properties of the mixture of NP and food powders.

Paste preparation by water supplementation to dry food powders is important in multiple situations in cooking and food processing. It is also important when 3D food printing is performed using a syringe- or screw-type extruder. We found that NP displays an activity to bind food granules (made of soybean and rice bran, as meat substitute) or powders (rice flour) for paste preparation at the water concentrations where binding is difficult without NP (Fig. S2; see J. Appl. Glycosci. Web site). Paste samples of vegetable powders in the presence of NP were dried to non-oil chips (Fig. S3; see J. Appl. Glycosci. Web site). Those chips exhibited hard and stable structures although they were shrunk and crooked a little, and they could be broken into two pieces by hands without crumbling into multiple particles (data not shown). We also found that NP reduced the adhesion of the sticky paste of soybean powders to a dish during its preparation (Fig. S4; see J. Appl. Glycosci. Web site).

Such NP binding activities could originate from interactions between NP and food powders in water. To approach the mechanism behind these interactions, we used RVA and two types of starchy powders, potato powders, and potato starch (Fig. 5). RVA is an instrument generally used for viscosity analysis of starchy powders with programmed tem-

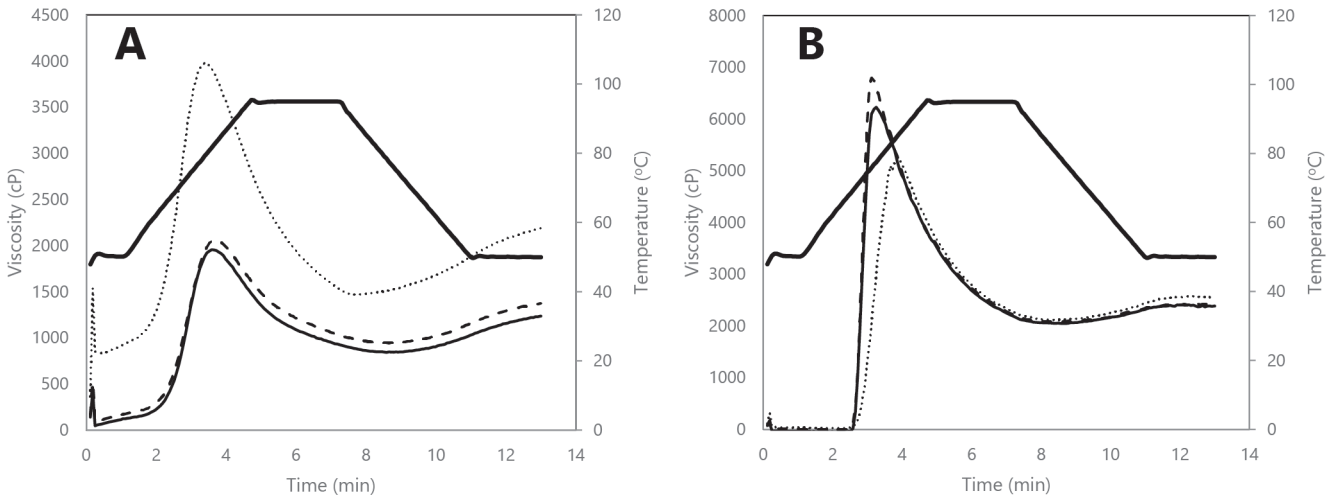

Fig. 5. Viscosity profiles of potato powders and potato starch in the presence of NP.

A, potato powders; B, potato starch. Solid lines, powders with water; broken lines, powders with BGL and water, dotted lines: powders with NP* and water; solid bold line, temperature profile.

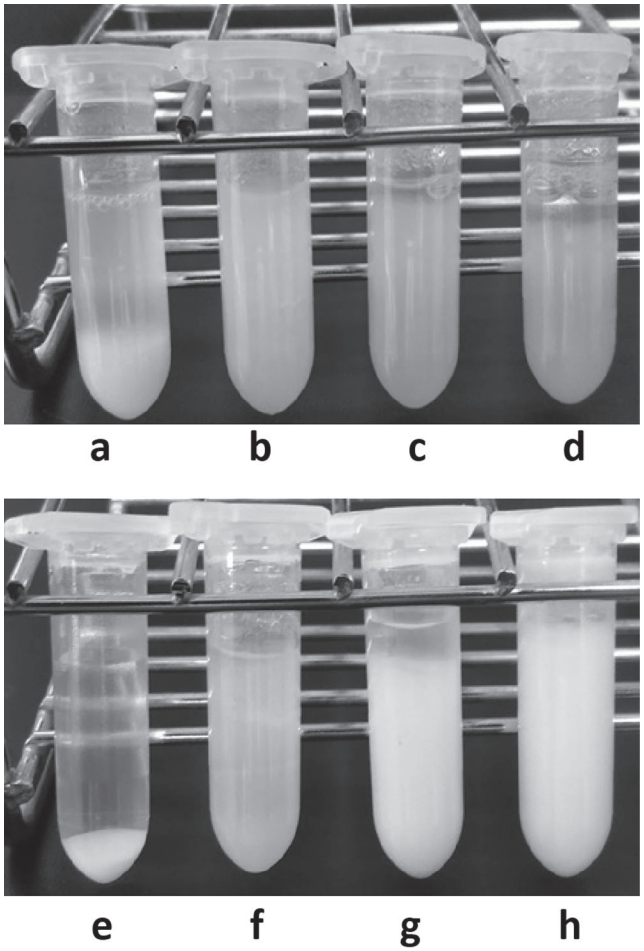

Fig. 6. Images of dispersed potato powders and potato starch in NP suspensions.

Tubes a–d, suspensions of potato powders; tubes e–h, suspensions of potato starch. To a tube with 1.4 mL of water (a) or NP* suspension (the solid content of 0.197 % (b), 0.049 % (c) or 0.012 % (d)), potato powder (50 mg) was added, the suspension was mixed well, and each tube was settled at room temperature for 1 h. As a different series, potato starch powder (50 mg (e, f) or 400 mg (g, h)) was added to a tube with 1.4 mL of water (e) or NP* suspension (the solid content of 0.197 % (f, g) or 0.388 % (h)), the suspension was mixed well, and each tube was also settled at room temperature for 1 h. Then, powder dispersions in the tubes were observed.

perature profiles as shown, which gelatinize, break down, and retrograde the starch to demonstrate unique profiles (Fig. 5, solid lines). NP supplementation in a slurry of potato powders significantly increased the initial viscosity, and the difference in the viscosity profile was basically stable during the whole measurement time, with a slight increase in peak viscosity (Fig. 5A, dotted line). The data suggest that strong interactions between potato powders and NP exist, which would cause the viscosity to increase. In contrast, potato starch slurry showed little viscosity increase upon NP supplementation, whereas a delay in peak time and lower peak viscosity could be observed (Fig. 5B, dotted line). It is speculated that, as reported for xanthan gum,[25] a high water-holding activity of NP would restrict or slow down the absorption of water by potato starch for gelatinization, which could also lead to a limited increase in the peak viscosity.

These two types of profiles suggest that potato starch granules exhibit no or very small interaction with NP compared with potato powders, and cell wall components in potato powder significantly affect that interaction. As described in a basic research study on plant cell walls and polysaccharides, cellulose readily interacts not only with BGL but also with arabinoxylan, xyloglucan, and pectin.[20)21)] At least in part, the NP binding activities on vegetable powders shown in Figs. S2–4 would be attributed to its interaction with the cell wall components.

Next, the dispersibilities of these powder samples in an NP* suspension (the solid content of 0.197 %) were visually characterized (Fig. 6). Both powder samples clearly precipitated in water (a and e in Fig. 6), whereas they remained dispersed in the presence of NP* (b–d and f–h in Fig. 6). Potato powders (50 mg) in 1.4 mL NP* (the solid content of 0.197 %) remained dispersed in the suspension without syneresis (b in Fig. 6), whereas syneresis on the top of the suspension could be observed in NP* suspensions of the solid contents of 0.049 and 0.012 % including the same powder amounts (c and d in Fig. 6, respectively). As potato powders absorb water and swell well to lower the apparent specific gravity closer to water, the addition of more potato powder in sample b in Fig. 6 resulted in a well-dispersed suspension overall without syneresis (data not shown). In the samples highlighted on c and d in Fig. 6, NP* suspensions at the lower concentrations resulted in high potato powder to the NP* particles ratios, which would form contracted network structures connected by potato powders in the suspension to induce syneresis.

In contrast, potato starch (50 mg), exhibiting weaker interactions with NP* (Fig. 5B), also appeared to be well-dispersed in 1.4 mL of NP* (the solid content of 0.197 %). When the amount of potato starch increased to 400 mg, the syneresis could be observed on the top of the suspension (g, Fig. 6), potentially attributed to the factors that the NP* network physically captured the potato starch powders, and dense starch granules with larger specific gravity than that of water pushed down the NP* network and induced the syneresis. When the solid NP* content increased to 0.388 %, no syneresis could be observed in the presence of 400 mg potato starch powder (h, Fig. 6). The reinforcement of the network with the additional NP* would mechanically strengthen the structure to maintain the powders.

According to the data of Figs. 5 and 6, the existence of two NP*-to-potato powder interaction types is suggested: a specific interaction between NP and cell wall components, and that of physical capture and holding of powders in the NP network. The former interaction would display a possibility to harden the powder paste with unique properties for new applications depending on the cell wall structures of the individual powders. The latter interaction would make it possible to disperse various particles in the NP suspension within appropriate ratios, which could stabilize the suspension properties, especially when syringe-type exclusion is used. For example, small bubbles of carbon dioxide were dispersed in a suspension made by mixing NP suspension with carbonated water (Fig. S5; see J. Appl. Glycosci. Web site). In addition, it is suggested that NP exhibits an activity to restrict or slow down the water transfer to the

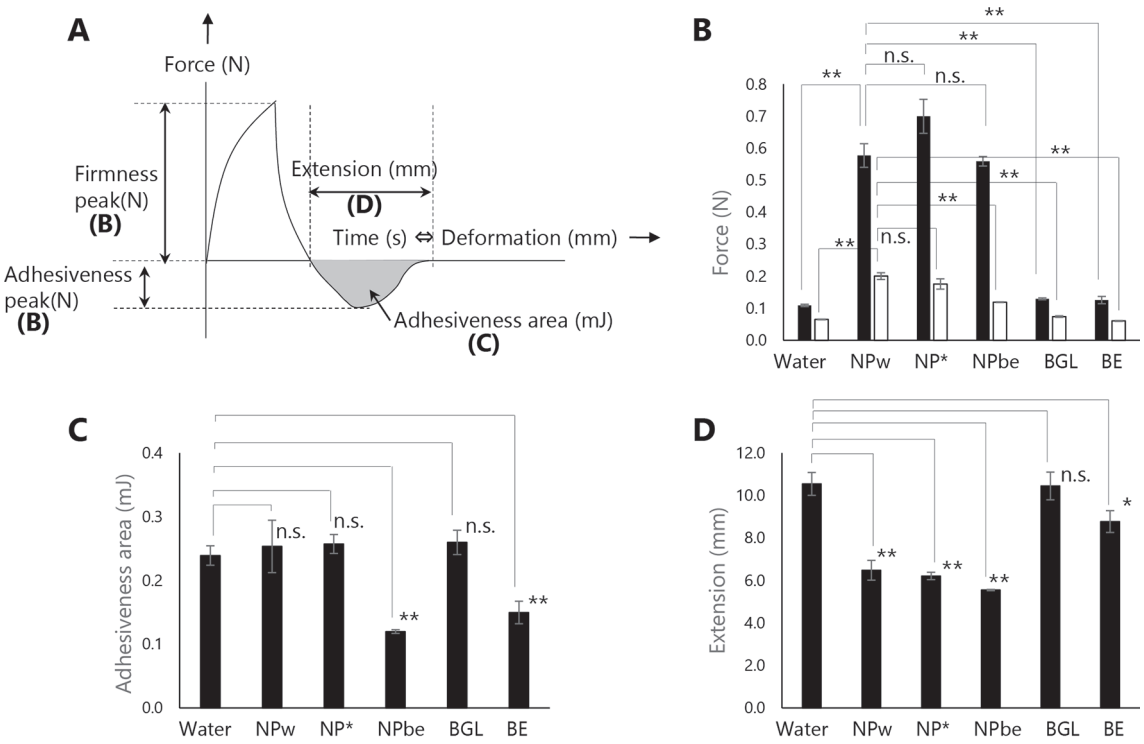

Fig. 7. Rheological parameters of potato paste samples with and without NP.

A: Schematic model of the force-displacement curve obtained from a single compression-extension test. The corresponding figure for a double compression-extension test by Park *et al*. (2014)[17] was slightly modified: the distance for extension (mm) used for this study was added, and the corresponding parameters for Fig. 7B–D are indicated as (**B**), (**C**), and (**D**), respectively.

B: firmness and adhesiveness peaks; black bars: firmness, white bars: adhesiveness, C: adhesiveness area, D: extension. The measurements were performed five times per dish by changing the press point on the surface one by one. Then, the average value excluding both the maximum and minimum values as outliers was calculated, and the average ± standard deviation of three plates was shown. Statistical analysis was performed using unpaired Student's *t*-test; $p < 0.05$ was considered statistically significant ($^{*}p < 0.05$, $^{**}p < 0.01$, n.s.; no significance).

powders (Fig. 5B). When water is mixed with dry food powders, rapid water absorption of parts of powders would result in lump production, turning the entire mixture heterogeneous. It is expected that NP could restrict or slow down the rapid water absorption of powders and promote homogeneous paste preparation.

Next, the rheological properties of the vegetable powder paste samples with and without NP were investigated (Fig. 7). We observed that the firmness peak value of the paste with NPw and NP* increased to 530 and 640 % of that with water, respectively (Fig. 7B). These increases would be mainly attributed to the presence of the disintegrated BC, a trend observed in the case of NPbe (510 % of that with water, Fig. 7B). In contrast, the adhesiveness area of the paste sample with water was equivalent to those with NPw, NP*, and the BGL solution, and it was higher than those with NPbe and BE suspension (Fig. 7C). The adhesiveness area is defined as the peak area below the baseline (Fig. 7A), suggesting that the value would reflect both the value in the vertical and lateral directions in Fig. 7A (*i.e.*, adhesiveness peak, white bar in Fig. 7B and extension, Fig. 7D, respectively). It appears that the adhesiveness peak values of samples with NPw, NP*, and NPbe (Fig. 7B) are larger than those with water and might somewhat reflect their firmness, whereas the corresponding extension values are lower than those with water (Fig. 7D). These trends would result in the large adhesiveness area values of the samples with NPw and NP*, and the smaller adhesiveness peak of that with NPbe would contribute to lower the adhesiveness area value (Fig. 7C). The BE exhibits unique properties in both forms of the NPbe and BE suspensions, reflected in the low adhesiveness area values (Fig. 7C). As BE is composed of multiple components including BGL and xylan, further evaluation studies would be required to approach the mechanism.

It is speculated that the NP* effect on lowering the soybean paste stickiness (Fig. S4) might be attributed to the difference in the extension values between the samples with water and NP* (Fig. 7D). The extension value indicates the time (and distance) needed for the separation of the lower face of the plunger from the surface of the sample, and the quick separation would reflect the low stretchiness of the paste to be split into smaller parts. In addition, the difference in the adhesiveness peak values in those two samples (Fig. 7B) might help keep the lumps of the paste compact instead of stretching, which would also reduce the transfer of parts of the paste to a dish or spatula in Fig. S4.

The effect of NP on raising the paste hardness can be applied for maintaining the printability at the lower powder concentration by a screw type 3D food printer. The paste sample of 20 % (w/w) potato powders in the presence of NPbe was successfully layered to form a cylinder structure as programmed, while the diameter was expanded by 30 % due to a crush of the bottom part by the weight of the upper part (Fig. 8A). The corresponding test with the paste without NP could not be performed as the paste was too soft

to maintain in the reservoir vessel, and it automatically spilled down from the nozzle of the vessel (data not shown). Instead, an image of the product with the harder paste of 22.5 % potato powder without NP was used for drawing a cylinder structure using the same program (Fig. 8B); the diameter of the bottom became larger to 195 % by a severe crush by the upper layers, suggesting that the hardness of the extruded paste at the bottom was not large enough to hold the upper layers. Therefore, using NP for paste preparation would extend the lower paste concentration limit which could widen the applicability of the powders to 3D food printing devices.

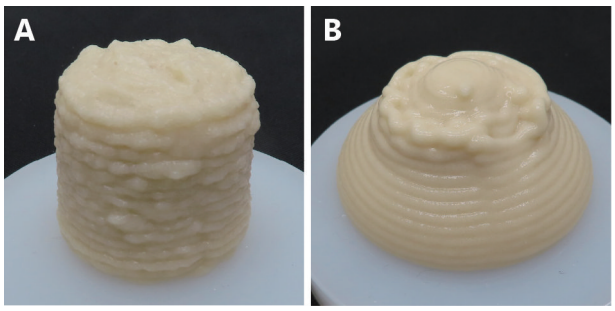

Fig. 8. Images of 3D printed products made of potato paste samples with and without NP.

A, excluded potato paste sample at 20 % (w/w) of powder content (with NPbe); B, excluded potato paste sample at 22.5 % (w/w) of powder content (without NPbe). A program for a cylinder structure was applied for production at room temperature.

Vegetables and fruits have been regarded as nonprintable with 3D food printers due to their innate characteristics, despite their significant nutritional and functional importance.[7)26)] Meanwhile, Kim *et al.* succeeded in the 3D printing of a programmed structure using paste samples of vegetable powders by 10 % of xanthan gum or hydroxypropyl methylcellulose supplementation.[27)] While this technology is expected to improve the applicability of various types of vegetable powders to 3D food printers, the use of high concentrations of hydrocolloids would lead to unified textures. As described in the Introduction section, it would be more desirable if individual food powders could express their own new textures to recognize and enjoy the various gifts of nature. The solid NP content used for 3D printing (Fig. 8A) in this study was 0.71 %, which is significantly lower than that of the hydrocolloid in the above-mentioned report. It is therefore expected that NP binds food powders to establish structures with low negative effects on the textures, which should be expressed by the powders.

Gel formation experiments.

In this study, we selected curdlan as a gel-forming polysaccharide to develop a new procedure for gelation by laser heating, as curdlan suspensions rapidly form gels by heating. Curdlan powders absorb water at room temperature, and the swelled powders in water were observed in a precipitated form (Fig. 9A, left tube). In contrast, the

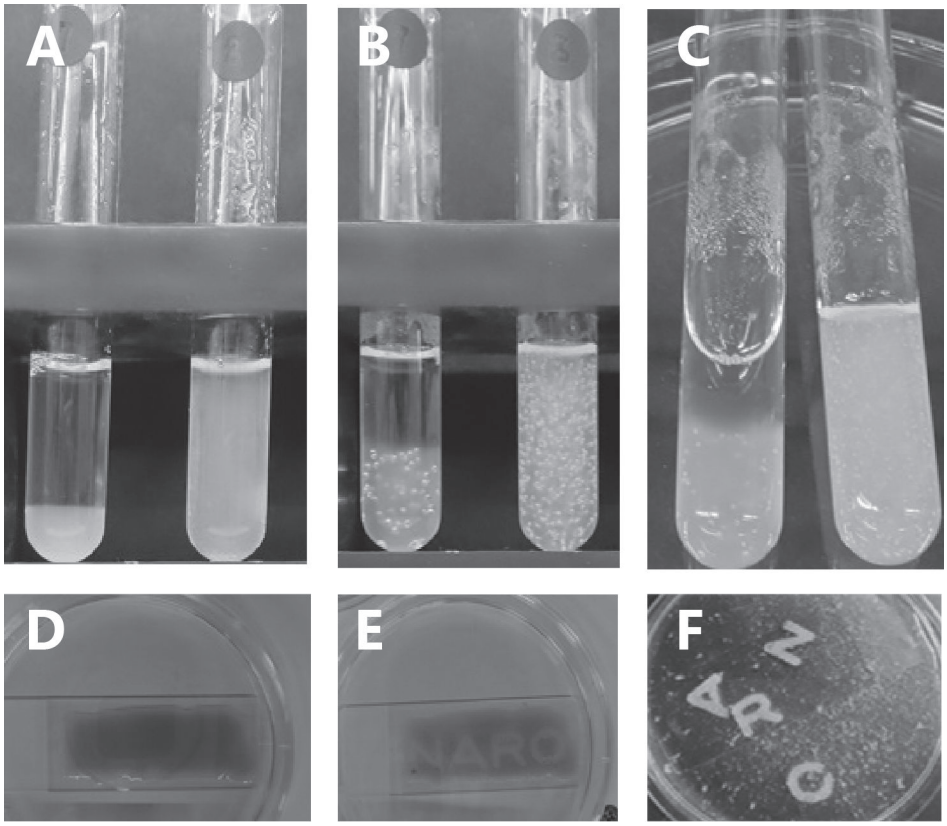

Fig. 9. Images of samples for curdlan gel formation with and without NP.

The suspensions in the left and right test tubes in A–C are composed of curdlan powders and water, and curdlan powders, NP*, and water (NP*/curdlan suspension), respectively. A, leaving for 1 min at room temperature after agitation; B, after heating at 85 ºC for 15 min and the subsequent cooling to room temperature; C, the tilted tubes in B to observe if fluidization occurred. D–F, images for a laser irradiation experiment of an NP*/curdlan suspension with turmeric powders. D, the suspension spread on a glass plate (before irradiation); E, after irradiation of D; and F, after rinsing of E.

swelled curdlan powders dispersed well with the aid of NP in the right tube in Fig. 9A. After heating both tubes at 85 ºC for 15 min, the precipitate in the left tube swelled further and formed a turbid part at the lower part of the suspension (Fig. 9B, left tube), whereas the whole suspension in the right tube in Fig. 9B was turbid. When these tubes were tilted after the heat treatment, the upper part of the suspension fluidized in the tube without NP (Fig. 9C, left tube), whereas the gel shape was maintained in the tube with NP (Fig. 9C, right tube). These results indicate that more homogeneous curdlan gel could be formed by heating without the agitation of the suspension when NP is used for curdlan powder dispersion.

The finding in the curdlan suspension with NP that agitation is unnecessary for gel formation from powders moved us on to the next experiment, hypothesizing that laser heating could induce the formation of small gel in a small, targeted area on the suspension settled on the stage for laser irradiation. As a blue laser light used in the study needs targets with appropriate colors that absorb the light to heat the suspension, we adopted turmeric powder as an edible coloring agent. A suspension of turmeric and curdlan powders was obtained in a well-dispersed form and spread on a glass plate (Fig. 9D). Then, the laser light was irradiated to draw four characters on the spread suspension (N,A,R, and O, Fig. 9E). It was confirmed after rinsing the glass plate with water that the irradiated parts were exclusively converted to gel (Fig. 9F). The laser irradiation was also performed using red paprika powders instead of turmeric powders (Fig. S6; see J. Appl. Glycosci. Web site).

Laser irradiation as a 3D food printing technology could be applied for selective sintering to form fine structures and textures.[26] However, selective laser sintering is only suitable for certain materials, such as sugar and fat-based materials. Our new gelation procedure with the aid of NP would help design precise and fine textures on the surface of the layer made of various food powders. In addition, the gel formation activities could be controlled not only with laser heating but also other heating methods, including blowing hot wind, layer-level heating by an infrared heater, and heating from the bottom of the layer. This process could be potentially applied for multiple lamination methods which have been used in 3D material printing, such as in the case of the stereolithography apparatus, or material and binder jetting methods.[28]

CONCLUSIONS

The control of the physical characteristics of pastes is expected to represent a breakthrough both for the resource management of agricultural products and for the field of the next-generation food industry. In this study, we described that NP modifies the binding- and adhesion properties of vegetable powder-derived paste samples and promotes food powder dispersion in the suspension. Further studies on the elucidation and control of NP and cell wall component interactions of the food powders would be necessary to provide the products with new properties and textures. The relevant information of polysaccharide-polysaccharide interactions could not only help us approach the roles of polysaccharides given by nature but could also be applied to the development of novel food- and non-food materials by exploiting the potential of various natural bio-resources.

CONFLICTS OF INTEREST

The authors declare no conflict of interests.

ACKNOWLEDGMENTS

This work was supported by Cabinet Office, Government of Japan, Cross-ministerial Moonshot Agriculture, Forestry and Fisheries Research and Development Program, (funding agency: Bio-oriented Technology Research Advancement Institution). We are grateful to Ms. Kana Hiramoto, Ms. Hiromi Nakayama, and Ms. Kazuyo Sato for their excellent technical assistance. The authors would like to thank Enago (www.enago.jp) for the English language review.

REFERENCES

1) FAO, IFAD, UNICEF, WFP, and WHO: The State of Food Security and Nutrition in the World 2020. Transforming food systems for affordable healthy diets. Rome, FAO (2020). https://doi.org/10.4060/ca9692en
2) K.M. Anser, T. Hina, S. Hameed, M.H. Nasir, I Ahmad, and M.A.R. Naseer: Modeling adaptation strategies against climate change impacts in integrated rice-wheat agricultural production system of Pakistan. *Int. J. Environ. Res. Public Health*, **17**, 2522 (2020).
3) R. Kanter and S. Boza: Strengthening local food systems in times of concomitant global crises: reflections from Chile. *Am. J. Public Health*, **110**, 971–973 (2020).
4) FAO: *The State of Food and Agriculture 2019*. *Moving forward on food loss and waste reduction*. Rome (2019). http://www.fao.org/3/ca6030en/ca6030en.pdf
5) C. Bas-Bellver, C. Barrera, N. Betoret, and L. Seguí: Turning agri-food cooperative vegetable residues into functional powdered ingredients for the food industry. *Sustainability*, **12**, 1284 (2020).
6) M.C. Karam, J. Petit, D. Zimmer, and E.B. Djantou: Effects of drying and grinding in production of fruit and vegetable powders: A review. *J. Food Eng.,* **188**, 32–49 (2016).
7) T. Pereira, S. Barroso, and M.M. Gil: Food texture design by 3D printing: A review. *Foods*, **10**, 320 (2021).
8) K. Nishinari: Texture and rheology in food and health. *Food Sci. Technol.*, **15**, 99–106 (2009).
9) F. Dourado, M. Gama, and A.C. Rodrigues: A review on the toxicology and dietetic role of bacterial cellulose. *Toxicol. Rep.*, **4**, 543–553 (2017).
10) H.M.C. Azeredo, H. Barud, C.S. Farinas, V.M. Vasconcellos, and A.M. Claro: Bacterial cellulose as a raw material for food and food packaging applications. *Front. Sustain. Food Syst*., **3**, 7 (2019).
11) A. Okiyama, M. Motoki, and S. Yamanaka: Bacterial cellulose IV. Application to processed foods. *Food Hydrocoll.*,

6, 503–511 (1993).
12) P. Paximada, E. Tsouko, N. Kopsahelis, and A.A. Koutinas: Bacterial cellulose as stabilizer of o/w emulsions. *Food Hydrocoll.*, **53**, 225–232 (2016).
13) Y. Guo, X. Zhang, W. Hao, Y. Xie, L. Chen, Z. Li, B. Zhu, and X. Feng: Nano-bacterial cellulose/soy protein isolate complex gel as fat substitutes in ice cream model. *Carbohydr. Polym.*, **198**, 620–630 (2018).
14) A. Okiyama, M. Motoki, and S. Yamanaka: Bacterial cellulose III. Development of a new form of cellulose. *Food Hydrocoll.*, **6**, 493–501 (1993).
15) D. Lin, R. Li, P. Lopez-Sanchez, and Z. Li: Physical properties of bacterial cellulose aqueous suspensions treated by high pressure homogenizer. *Food Hydrocoll.*, **44**, 435–442 (2015).
16) F. Hayakawa, A. Fukui, J. Matsuki, and H. Yano: Effect of glutathione on the physical properties of soy dough. *Bull. NARO, Food Res.,* **1**, 1–7 (2017) (In Japanese).
17) I. Park, S.-H. Kim, I.-M. Chung, I.-H. Kim, C.F. Shoemaker, and Y.-S. Seo: Comparison of a dynamic test to analyze the texture of cooked rice with a classic compression - extension test. *Starch/Stärke,* **66**, 998–1004 (2014).
18) K. Watanabe, M. Tabuchi, Y. Morinaga, and F. Yoshinaga: Structural features and properties of bacterial cellulose produced in agitated culture. *Cellulose*, **5**, 187–200 (1998).
19) D. Mikkelsen, M.J. Gidley, and B.A. Williams: *In vitro* fermentation of bacterial cellulose composite as model dietary fibers. *J. Agric. Food Chem.*, **59**, 4025–4032 (2011).
20) D. Mikkelsen, B.M. Flanagan, S.M. Wilson, A. Bcic, and M.J. Gidley: Interaction of arabinoxylan and (1,3)(1,4)-β-glucan with cellulose networks. *Biomacromolecules*, **16**, 1232–1239 (2015).
21) S.N. Kiemle, X. Zhang, A.R. Esker, G. Toriz, P. Gatenholm, and D.J. Cosgrove: Role of (1,3)(1,4)-β-glucan in cell walls: interaction with cellulose. *Biomacromolecules*, **15**, 1727–1736 (2014).
22) J.C. Muñoz-García, K.R. Corbin, H. Hussain, V. Gabrielli, T. Koev, D. Iuga, A.N. Round, D. Mikkelsen, P.A. Gunning, F.J. Warren, and Y.Z. Khimyak: High molecular weight mixed-linkage glucan as a mechanical and hydration modulator of bacterial cellulose: characterization by advanced NMR spectroscopy. *Biomacromolecules*, **20**, 4180–4190 (2019).
23) S.-C. Chang, R.K. Saldivar, P.-H. Liang, and Y.S.Y. Hsieh: Structures, biosynthesis, and physiological functions of (1,3;1,4)-β-D-glucans. *Cells*, **10**, 510 (2021).
24) E.J. Murphy, E. Rexoagli, I. Major, N.J. Rowan, and J.G. Laffey: β-Glucan metabolic and immunomodulatory properties and potential for clinical application. *J. Fungi*, **6**, 356 (2020).
25) M. Belorio, G. Marcondes, and M. Gómez: Influence of psyllium *versus* xanthan gum in starch properties. *Food Hydrocoll.*, **105**, 105843 (2020).
26) J. Sun, W. Zhou, D. Huang, J.Y.H. Fuh, and G.S. Hong: An overview of 3D printing technologies for food fabrication. *Food Bioprocess Technol.*, **8**, 1605–1615 (2015).
27) H.W. Kim, J.H. Lee, S.M. Park, M.H. Lee, I.W. Lee, H.S. Doh, and H.J. Park: Effect of hydrocolloids on rheological properties and printability of vegetable inks for 3D food printing. *J. Food Sci.*, **83**, 2923–2932 (2018).
28) L.-Y. Zhou, J. Fu, and Y. He: A review of 3D printing technologies for soft polymer materials. *Adv. Funct. Mater.*, **30**, 200187 (2020).